ANTIOXIDANTS & REDOX SIGNALING
Volume 38, Numbers 16–18, 2023

DOI: 10.1089/ars.2022.0034

ORIGINAL RESEARCH COMMUNICATION

Peroxiredoxin-4 and Dopamine D5 Receptor Interact to Reduce Oxidative Stress and Inflammation in the Kidney

Bibhas Amatya,[1] Sufei Yang,[2,3] Peiying Yu,[2,4] Pedro A.S.Vaz de Castro,[1] Ines Armando,[1,2,4] Chunyu Zeng,[3] Robin A. Felder,[5] Laureano D. Asico,[1,2,4] Pedro A. Jose,[1,2,4,6] and Hewang Lee[1,2,4]

Abstract

Aims: Reactive oxygen species are highly reactive molecules generated in different subcellular compartments. Both the dopamine D5 receptor (D_5R) and endoplasmic reticulum (ER)-resident peroxiredoxin-4 (PRDX4) play protective roles against oxidative stress. This study is aimed at investigating the interaction between PRDX4 and D_5R in regulating oxidative stress in the kidney.

Results: Fenoldopam (FEN), a D_1R and D_5R agonist, increased PRDX4 protein expression, mainly in non-lipid rafts, in D_5R-HEK 293 cells. FEN increased the co-immunoprecipitation of D_5R and PRDX4 and their colocalization, particularly in the ER. The efficiency of Förster resonance energy transfer was increased with FEN treatment measured with fluorescence lifetime imaging microscopy. Silencing of *PRDX4* increased hydrogen peroxide production, impaired the inhibitory effect of FEN on hydrogen peroxide production, and increased the production of interleukin-1β, tumor necrosis factor (TNF), and caspase-12 in renal cells. Furthermore, in *Drd5*$^{-/-}$ mice, which are in a state of oxidative stress, renal cortical PRDX4 was decreased whereas interleukin-1β, TNF, and caspase-12 were increased, relative to their normotensive wild-type *Drd5*$^{+/+}$ littermates.

Innovation: Our findings demonstrate a novel relationship between D_5R and PRDX4 and the consequent effects of this relationship in attenuating hydrogen peroxide production in the ER and the production of proinflammatory cytokines. This study provides the potential for the development of biomarkers and new therapeutics for renal inflammatory disorders, including hypertension.

Conclusion: PRDX4 interacts with D_5R to decrease oxidative stress and inflammation in renal cells that may have the potential for translational significance. *Antioxid. Redox Signal*. 38, 1150–1166.

Keywords: dopamine D5 receptor, endoplasmic reticulum, inflammation, peroxiredoxin-4, reactive oxygen species

Introduction

REACTIVE OXYGEN SPECIES (ROS) are a family of oxygen-containing reactive molecules (Qaddumi and Jose, 2021) that play important roles in diverse physiological and pathophysiological processes, including inflammatory immune responses (Mittal et al, 2014). A prototypical role of ROS is the killing of phagocytosed bacteria through nicotinamide adenine dinucleotide phosphate (NADPH) oxidase activation.

[1]Department of Medicine, The George Washington University School of Medicine & Health Sciences, Washington, District of Columbia, USA.
[2]Division of Nephrology, Department of Medicine, University of Maryland School of Medicine, Baltimore, Maryland, USA.
[3]Department of Cardiology, Daping Hospital, The Third Military Medical University, Chongqing, China.
[4]Center for Molecular Physiology Research, Children's National Medical Center, Washington, District of Columbia, USA.
[5]Department of Pathology, University of Virginia Health Sciences Center, Charlottesville, Virginia, USA.
[6]Department of Pharmacology/Physiology, The George Washington University School of Medicine & Health Sciences, Washington, District of Columbia, USA.

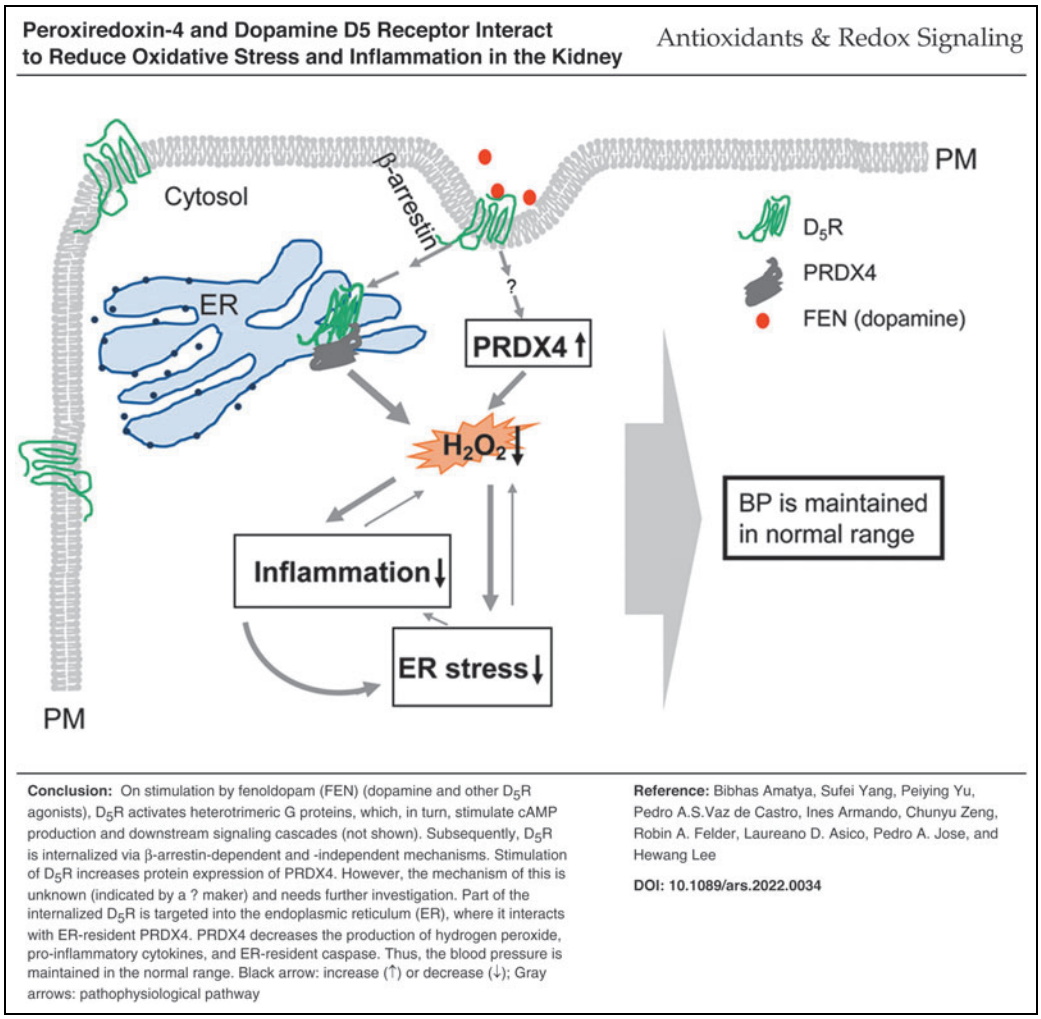

However, overly increased ROS levels are implicated in the pathogenesis of a wide variety of disorders, such as cancers, cardiovascular diseases, including hypertension, acute and chronic kidney diseases, and neurodegenerative diseases (Harris and DeNicola, 2020; Singh et al, 2019a; Xiao and Harrison, 2020). Cells produce and compartmentalize ROS production in certain subcellular sites, such as the mitochondria and endoplasmic reticulum (ER), for cell-site specific effects and minimize their detrimental effects in a limited area (Castro et al, 2021; Kakihana et al, 2012).

The dopamine D5 receptor (D_5R), one of the dopamine D1-like receptors, is a G protein-coupled receptor (GPCR) with high affinity to dopamine that signals *via* the $G\alpha_s/G\alpha_{olf}$ and 3',5'-cyclic adenosine monophosphate/protein kinase A (cAMP/PKA) pathway (Beaulieu and Gainetdinov, 2011). The D_5R can also couple to Gαq and the phospholipase C pathway (Gildea et al, 2014; Undieh, 2010). Mice with germline deletion of the D_5R gene ($Drd5^{-/-}$) are hypertensive (Hollon et al, 2002; Lee et al, 2021; Lu et al, 2013; Zeng et al, 2009; Zhang and Harris, 2015).

The ROS production in the kidney and brain is greater in $Drd5^{-/-}$ mice than their $Drd5^{+/+}$ littermates (Qaddumi and Jose, 2021; Yang et al, 2006). D_5R exerts its antioxidant properties through the inhibition of ROS production from NADPH oxidases (Yang et al, 2015; Yang et al, 2006) and mitochondria (Lee et al, 2021). In addition, the oxidative stress in $Drd5^{-/-}$ mice can be related to the decrease and dysfunction of a variety of antioxidant enzymes that scavenge ROS (Qaddumi and Jose, 2021).

Thus, D_5R decreases ROS production through the increase in the activity and expression of antioxidant enzymes, such as

Innovation

This study demonstrates for the first time that dopamine D5 receptor (D_5R), independent of the dopamine D1 receptor, exerts its antioxidant properties in the endoplasmic reticulum by increasing the protein expression of and interaction with peroxiredoxin-4 (PRDX4). *PRDX4* silencing increased the production of hydrogen peroxide, proinflammatory cytokines, and ER stress-associated caspase-12 and also impaired the inhibitory effect of D_5R in these processes. This study has translational potential since relative to $Drd5^{+/+}$ mice, the renal cortical PRDX4 protein expression is decreased in $Drd5^{-/-}$ mice, which are in a state of oxidative stress. Thus, PRDX4 has the potential for the development of biomarkers and new therapeutics for renal inflammatory diseases, including hypertension.

heme oxygenase-1 (Lu et al, 2013), paraoxonase 2 (Yang et al, 2015), and thioredoxin (Wang et al, 2019) in the kidney. Peroxiredoxins (PRDXs), a ubiquitous family of antioxidant enzymes, regulate ROS using thioredoxin as an electron donor. However, it is not known whether D_5R decreases ROS production through PRDXs.

PRDXs are thiol-specific antioxidant enzymes that detoxify ROS by oxidizing their cysteine groups to cysteine sulfinic acid (Cys-SO_2H) or cysteine sulfonic acid (Cys-SO_3H) (Bolduc et al, 2021). Six PRDXs have been identified; they are ubiquitously expressed, playing multiple physiological functions (Bolduc et al, 2021). PRDX4, a prototype 2-cys PRDX subgroup and the only PRDX found in the ER, contains a hydrophobic signal sequence at the N-terminus that is responsible for its ER localization and secretion into the extracellular space (Abbasi et al, 2012). The ER has more oxidizing actions than the cytosol (Bolduc et al, 2021; Kakihana et al, 2012).

The ER is critical in the folding of membrane and secretory proteins, during which oxidative protein folding is achieved in association with luminal hydrogen peroxide production (Kakihana et al, 2012). In addition to the oxidative system, the ER also contains the reductase system that dynamically regulates the redox state. The important reductases in ER are glutathione peroxidases 7 and 8 and PRDX4 (Kakihana et al, 2012).

PRDX4 regulates redox balance by reducing hydrogen peroxide into water; PRDX4 is the most highly expressed hydrogen peroxide-scavenging protein in the ER in humans (Bolduc et al, 2021; Elko et al, 2021). *PRDX4* overexpression decreases whereas *PRDX4* silencing increases ROS production and ER stress (Konno et al, 2021). PRDX4 expression is altered in several pathophysiological conditions, including inflammation (Lipinski et al, 2019) and chronic inflammation-related diseases, such as atherosclerosis, cancer, chronic kidney disease, and type 2 diabetes (Abbasi et al, 2012). The importance of PRDX4 in the immune response has been demonstrated in mammals and fishes.

In *Prdx4* transgenic mice, the expression of many inflammatory factors, including interleukin (IL)-1β, tumor necrosis factor (TNF), TNF receptor, toll-like receptors, and nuclear factor kappa-light-chain-enhancer of activated B cells (NF-κB), is suppressed; these mice are also protected from oxidative stress (Yamada and Guo, 2018). By contrast, *Prdx4* knockout mice have increased susceptibility to oxidative damage (Iuchi et al, 2009). In the fish, PRDX4 is upregulated by bacterial challenge whereas *prdx4* gene knockdown increases the expression of proinflammatory cytokines and chemokines and decreases the expression of an anti-inflammatory interleukin, IL-10 (Valero et al, 2015).

Our studies show that PRDX4, as an ER antioxidant enzyme, interacts with D_5R. This interaction regulates its protein expression and impairs hydrogen peroxide and inflammatory cytokine production in kidney cells.

Results

Activation of D_5R increases PRDX4 protein expression in D_5R-human embryonic kidney 293 cells

FEN (25 n*M*, 12 h), a D1-like receptor (D_1R and D_5R) agonist (Gildea et al, 2014; Gildea et al, 2008; Lee et al, 2021; Li et al, 2009; Li et al, 2008; Lu et al, 2013; Sanada et al, 1999; Wang et al, 2019; Yang et al, 2015; Yang et al, 2006; Yu et al, 2014), increased PRDX4 protein expression in nonreducing (Fig. 1A) and reducing conditions (Fig. 1B). Monomeric, dimeric, and oligomeric forms of PRDX4 were increased by FEN treatment (Fig. 1A, B) but only monomers were observed in reducing conditions (Fig. 1B) in human embryonic kidney 293 (HEK293) cells heterologously expressing D_5R (D_5R-HEK293). The presence of oligomeric and dimeric forms of PRDX4 in nonreducing conditions and the monomeric form of PRDX4 in reducing conditions is consistent with previous observations in mouse lung epithelial cells (Elko et al, 2021).

HEK293 cells do not endogenously express D_1R or D_5R (Lee et al, 2021; Lu et al, 2013; Yang et al, 2015; Yang et al, 2006). The specificity of the FEN effect on PRDX4 protein expression in D_5R-HEK293 cells was confirmed by SCH 39166 (SCH), a specific D1-like receptor (D_1R and D_5R) antagonist (Tice et al, 1994). Thus, the FEN-mediated increase in PRDX4 protein expression was prevented by SCH (1 μM), whereas SCH, by itself, had no effect on PRDX4 protein expression (Fig. 1). Furthermore, the protein expression of PRDX4, both dimer and monomer, in either nonreducing (Fig. 1C) or reducing (Fig. 1D) conditions, was not significantly altered by FEN treatment in D_1R-HEK293 cells, indicating a specific effect of D_5R on PRDX4 expression.

Activation of D_5R alters PRDX4 micromembrane distribution

Plasma membrane microdomains have crucial roles in receptor signaling, protein trafficking, degradation, and protein expression (Crul and Maléth, 2021; Martinez et al, 2020). FEN stimulation alters the distribution of GPCRs (*e.g.,* D_1R and D_5R) (34, 64), and non-GPCRs (*e.g.,* adenylyl cyclases, NADPH oxidases) (Li et al, 2009; Yang et al, 2006) in plasma membrane microdomains. Therefore, we studied the distribution of PRDX4 in membrane microdomains.

In the basal state, PRDX4 was distributed in both lipid rafts (LRs) and non-LRs, but to a greater extent in non-LRs (75.1% ± 11.4%) than LRs (24.9% ± 11.4%). FEN increased the distribution of PRDX4 mainly in non-LRs (LR: 30.9% ± 13.9%, non-LR: 174.1% ± 16.7%) (Fig. 2). Treatment with the cholesterol-depleting drug methyl-β-cyclodextrin (M-β-CD), which disrupts LRs (Li et al, 2009), resulted in the redistribution of PRDX4 to non-lipid raft (non-LR) microdomain (Fig. 2). The LRs and non-LRs are present in ERs, as in plasma membranes (Wang et al, 2020). The contact sites between the ER and plasma membrane serve to compartmentalize cAMP signaling (Crul and Maléth, 2021). However, our current studies did not determine the expression of PRDX4 in LRs and non-LRs exclusively in the ER.

D_5R interacts with PRDX4

To evaluate the potential interaction between D_5R and PRDX4, co-immunoprecipitation studies were performed. In the basal state, the D_5R co-immunoprecipitated with PRDX4; FEN (25 n*M*, 12 h) treatment increased the co-immunoprecipitation of D_5R and PRDX4 monomers and dimers in D_5R-HEK293 cells (Fig. 3A, B). In addition, treatment with D_1R/D_5R antagonist SCH prevented the ability of FEN to increase the co-immunoprecipitation of D_5R and PRDX4 (Fig. 3A, B). These results indicated that the

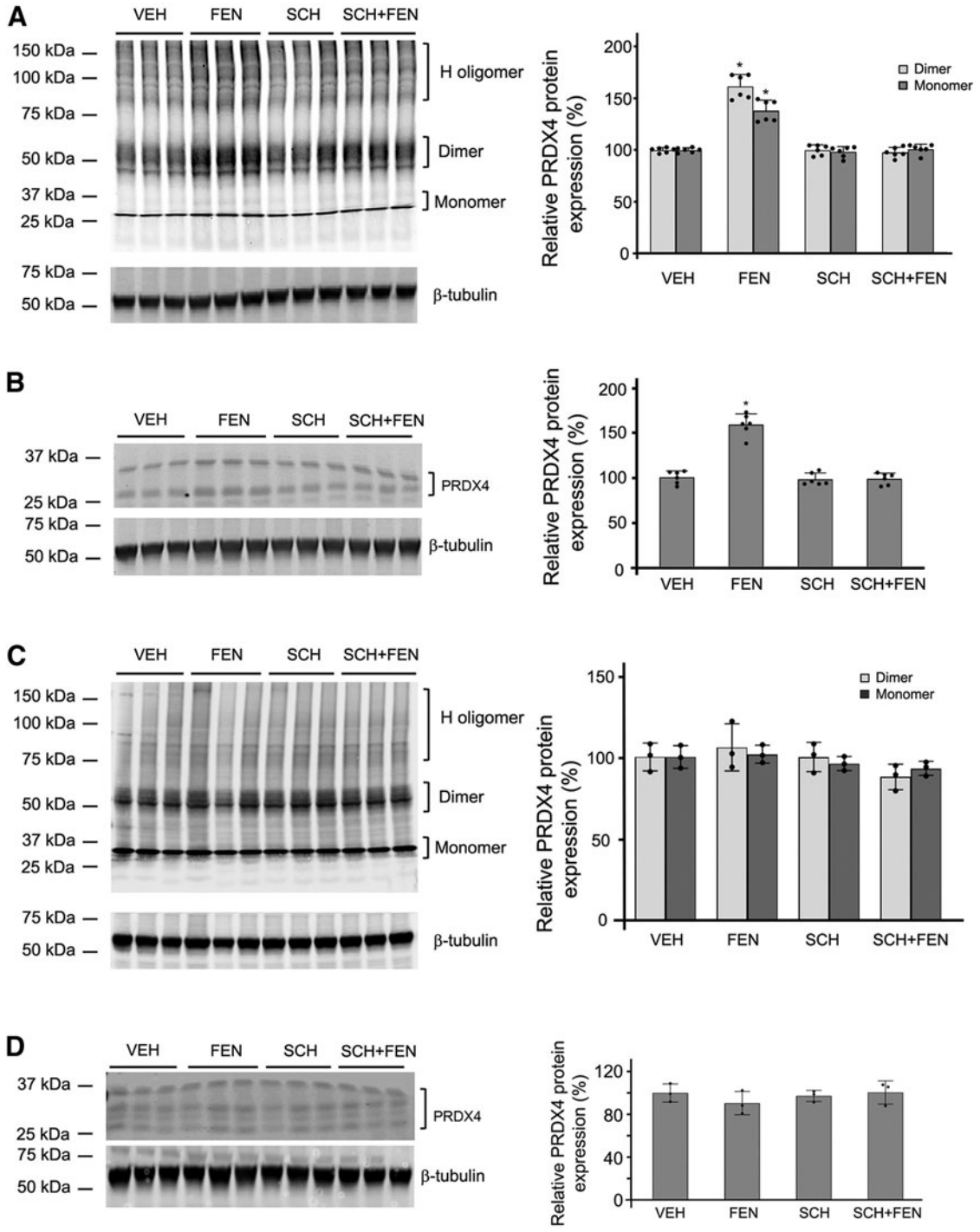

FIG. 1. PRDX4 protein expression in D_5R-HEK293 (A, B) and D_1R-HEK293 (C, D) cells. D_5R-HEK293 and D_1R-HEK293 cells were treated with the D_1R/D_5R agonist, FEN (25 n*M*, 12 h) in the absence or presence of the D_1R/D_5R antagonist, SCH (1 μM, 12 h), as indicated. The cell pellets were harvested, and the cell lysates were prepared in non-reducing **(A, C)** or reducing **(B, D**, 5% 2- mercaptoethanol) Laemmli buffer for 10% SDS-PAGE. β-tubulin was used for loading control. PRDX4 protein expression, determined by immunoblotting, is increased by FEN treatment. Monomers, dimers, and high-molecular-weight oligomers of PRDX4 are seen in non-reducing condition **(A, C)** but only monomers in reducing conditions **(B, D)**. H Oligomer, high-molecular-weight oligomerized form of PRDX4. **(A, B)** $n = 6$/group, **(C, D)** $n = 3$/group, $^*p < 0.05$ *versus* VEH, SCH, and SCH+FEN, one-way ANOVA, Newman–Keuls test. PRDX4, peroxiredoxin 4; FEN, fenoldopam; SCH, SCH39166; SDS-PAGE, sodium dodecyl sulfate-polyacrylamide gel electrophoresis; HEK293, human embryonic kidney 293.

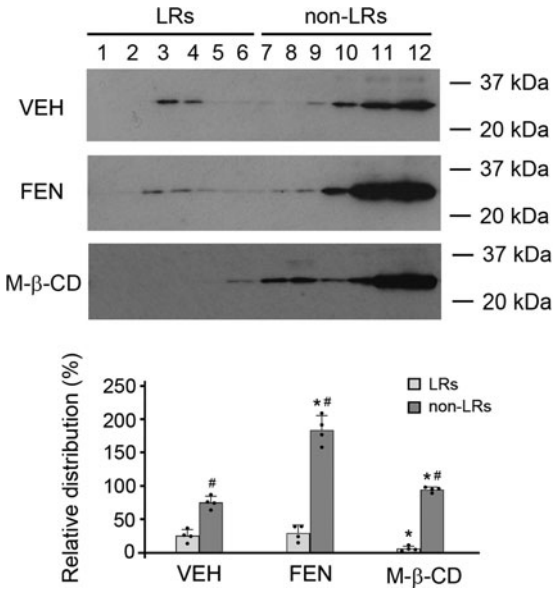

FIG. 2. Increase in PRDX4 protein expression in non-LR fractions with FEN treatment. D_5R-HEK293 cells were treated with the D_1R/D_5R agonist, FEN (25 n*M*, 12 h) or M-β-CD to disrupt LR microdomains. The membrane-enriched pellets were then subjected to sucrose gradient ultracentrifugation, and 12 fractions were obtained. The most buoyant fractions (fractions 1–6) represent LRs, whereas the rest (fractions 7–12) represent non-LRs. $n = 4$/group, $^*p < 0.05$ *versus* VEH, $^{\#}p < 0.05$ *versus* LRs, one-way ANOVA, Newman–Keuls test. LRs, lipid rafts; non-LRs, non-lipid rafts; M-β-CD, methyl-β-cyclodextrin.

FEN-mediated increase in the co-immunoprecipitation between D_5R and PRDX4 was through the activation of D_5R.

Consistent with the co-immunoprecipitation data, D_5R and PRDX4 colocalized in D_5R-HEK 293 cells (Fig. 3C). In the basal state, D_5R was distributed in the plasma membrane and intracellular compartments. By contrast, PRDX4 was scattered throughout the cytoplasm in intracellular membranes and punctuate vesicles of varying sizes with minimal colocalization with D_5R. However, FEN (25 n*M*, 12 h) markedly increased the colocalization between D_5R and PRDX4, particularly within the cytoplasm, presumably including ER (Fig. 3C). The effect of FEN was blocked by SCH, which by itself had no effect (Fig. 3C).

Since PRDX4 is an ER resident antioxidant and FEN increased D_5R co-localization with PRDX4, we studied the distribution of D_5R in ER with and without FEN stimulation. In the basal state, some D_5Rs resided in the ER but their colocalization was increased by the treatment with FEN (Fig. 4). Their colocalization in the ER was verified by calnexin, a commonly used ER marker (Schrag et al, 2001). The FEN treatment for 12 h increased the colocalization of D_5R and calnexin (Fig. 4). The effect of FEN was blocked by SCH, which by itself had no effect, in D_5R-HEK293 cells (Fig. 4).

To determine the physiological importance of the interaction between PRDX4 and D_5R and its relevance to renal physiology and role in hypertension, we performed co-immunoprecipitation and colocalization studies using human renal proximal tubule cells (hRPTCs), which endogenously express both proteins. Similar to what was found in D_5R-HEK293 cells, in hRPTCs, FEN stimulation increased the co-immunoprecipitation (Supplementary Fig. S1) and co-localization (Supplementary Fig. S2) of D_5R and PRDX4, and the residence of D_5R in the ER (Supplementary Fig. S3).

To investigate further the interaction between D_5R and PRDX4, fluorescence lifetime imaging-Förster resonance energy transfer (FLIM-FRET) microscopy was employed because this method is less influenced by fluorophore variations and photobleaching, and less prone to signal cross-contamination (Sun et al, 2013). In D_5R-HEK293 cells, FEN stimulation significantly shortened the quench time of D_5R with a significant increase in FRET efficiency from $\sim$18.67% (vehicle or VEH) to $\sim$26.95% (FEN) in the cytoplasmic regions of interest (Fig. 5).

Consistent with the colocalization and co-immunoprecipitation studies (Fig. 3), the increase in FRET efficiency was attenuated by SCH (1 μM, 30 min pretreatment); SCH, by itself, had no effect (SCH: $\sim$18.16%, SCH+FEN: $\sim$17.61%) (Fig. 5).

ROS production is increased by PRDX4 knockdown

As determined by the amount of hydrogen peroxide secreted into the culture medium, FEN (25 n*M*,12 h) decreased ROS production in both D_5R-HEK293 cells (VEH: 100.0% $\pm$ 9.7%, FEN:65.8% $\pm$ 11.2%, $n = 4$, Fig. 6A) and hRPTCs (VEH: 100.0% $\pm$ 15.1%, FEN: 55.2% $\pm$ 7.2%, $n = 4$, Fig. 6B) transfected with the scrambled siRNA. The inhibition of hydrogen peroxide production by FEN was not complete, consistent with our previous report that a certain amount of hydrogen peroxide is necessary to maintain cellular redox homeostasis (Cuevas et al, 2020). The inhibitory effect of FEN on hydrogen peroxide production was prevented by the pretreatment with SCH, which by itself had no effect (Fig. 6); the constitutive activity of D_5R (Hollon et al, 2002; Lee et al, 2021; Yang et al, 2006) was not observed in this experimental condition.

In the D_5R-HEK293 cells, the amount of hydrogen peroxide secreted into the culture medium was increased by *PRDX4* siRNA, from 100% $\pm$ 9.7% to 155.8% $\pm$ 22.0% (Fig. 6A). The inhibitory effect of FEN on hydrogen peroxide production was markedly impaired and became insignificant in *PRDX4* siRNA-treated D_5R-HEK293 cells (Fig. 6A). Similarly, in hRPTCs, hydrogen peroxide secreted into the culture medium was increased by *PRDX4* siRNA and the inhibitory effect of FEN also became insignificant (Fig. 6B). These results indicate that the silencing of *PRDX4* by its specific siRNA markedly increases hydrogen peroxide production and impairs the inhibitory effect of FEN on hydrogen peroxide production.

Proinflammatory cytokines are increased by PRDX4 knockdown

PRDX4 plays an important role in inhibiting the inflammatory responses (Lipinski et al, 2019) and oxidative stress, which can cause inflammation and vice versa (Qaddumi and Jose, 2021; Sun et al, 2021; Xiao and Harrison, 2020; Zhang and Harris, 2015). Therefore, it was essential to evaluate the effect of PRDX4 on the production of proinflammatory cytokines.

In D_5R-HEK293 cells, the siRNA-induced silencing of *PRDX4* increased the production of IL-1β from 100.0 $\pm$ 14.3% to 172.6 $\pm$ 15.7% ($n = 3$/group) and TNF from 100 $\pm$ 5.0% to 205.9 $\pm$ 13.7% ($n = 4$/group) (Fig. 7); *PRDX4*

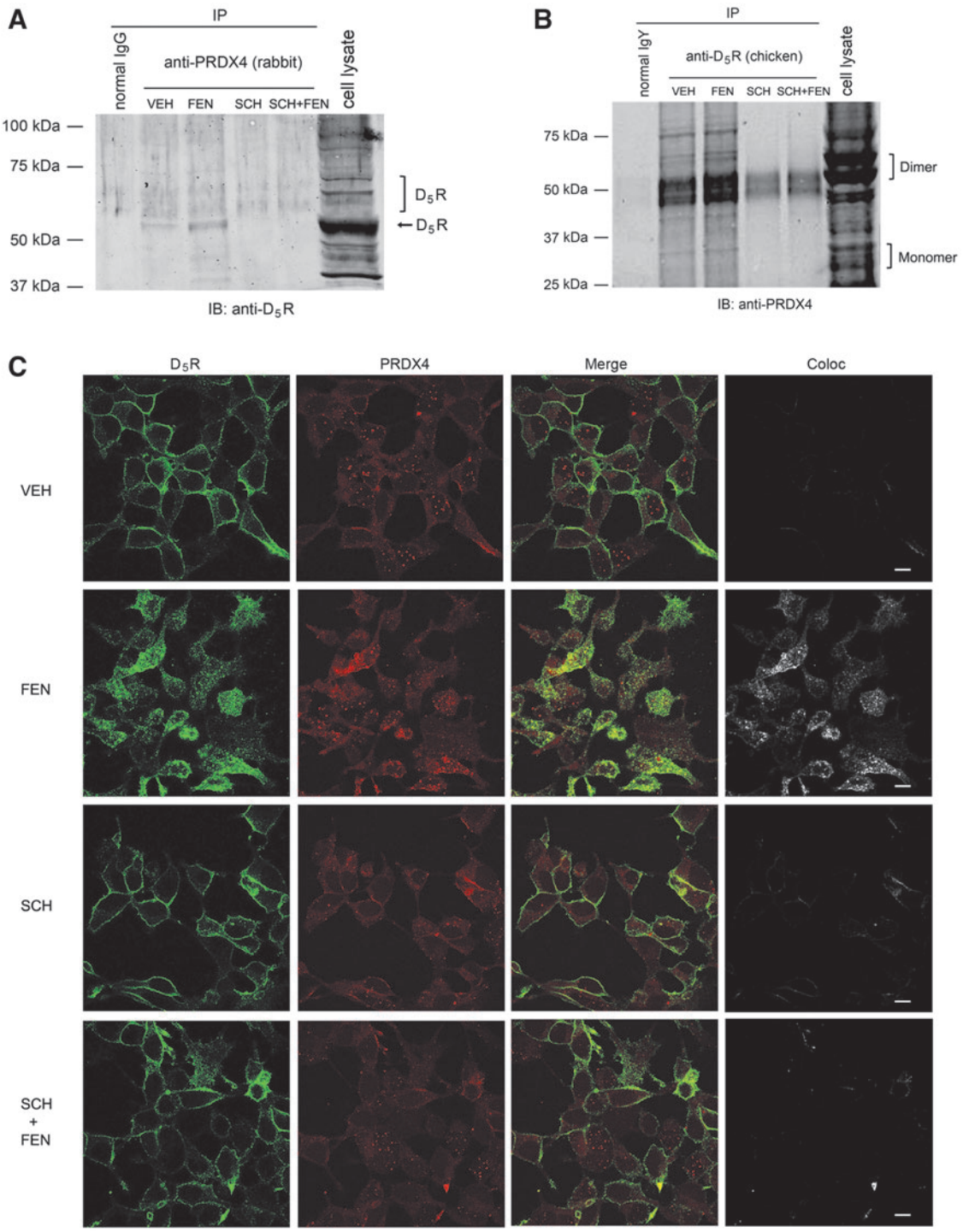

FIG. 3. Co-immunoprecipitation of PRDX4 and D_5R and their colocalization in D_5R-HEK293 cells. The D_5R-HEK293 cells were treated with VEH or the D_1R/D_5R agonist, FEN (25 n*M*, 12 h), in the absence or presence of the D_1R/D_5R antagonist, SCH (1 μM, 12 h), as indicated. The cell lysates were immunoprecipitated (IP) with anti-PRDX4 antibodies **(A)** or with anti-D_5R antibodies **(B)** coupled to Dynabeads for 4 h at 4°C. The protein complexes bound to the beads were eluted and prepared with non-reducing Laemmli buffer and separated by 10% SDS-PAGE, transferred onto nitrocellulose membranes, and immunoblotted (IB) with anti-D_5R antibodies **(A)** or anti-PRDX4 antibodies **(B)**. Normal IgY or IgG was used for negative control and immunoblotting of D_5R-HEK293 cell lysates for positive control. The blots are representatives of two independent experiments for **(A, B)**. **(C)** The cells were treated with VEH, FEN (25 n*M*, 12 h), in the absence or presence of SCH (1 μM, 12 h), as indicated. The cells were then immunostained with anti-D_5R (*green*) and anti-PRDX4 (*red*) antibodies. Co-localization (*yellow*) between D_5R and PRDX4 was increased by FEN treatment that was blocked by SCH treatment, which by itself had no effect. $n = 3$/group. A panel of separate colocalization images in ''Coloc'' were generated as described in the Methods section. Scale bar, 10 μm.

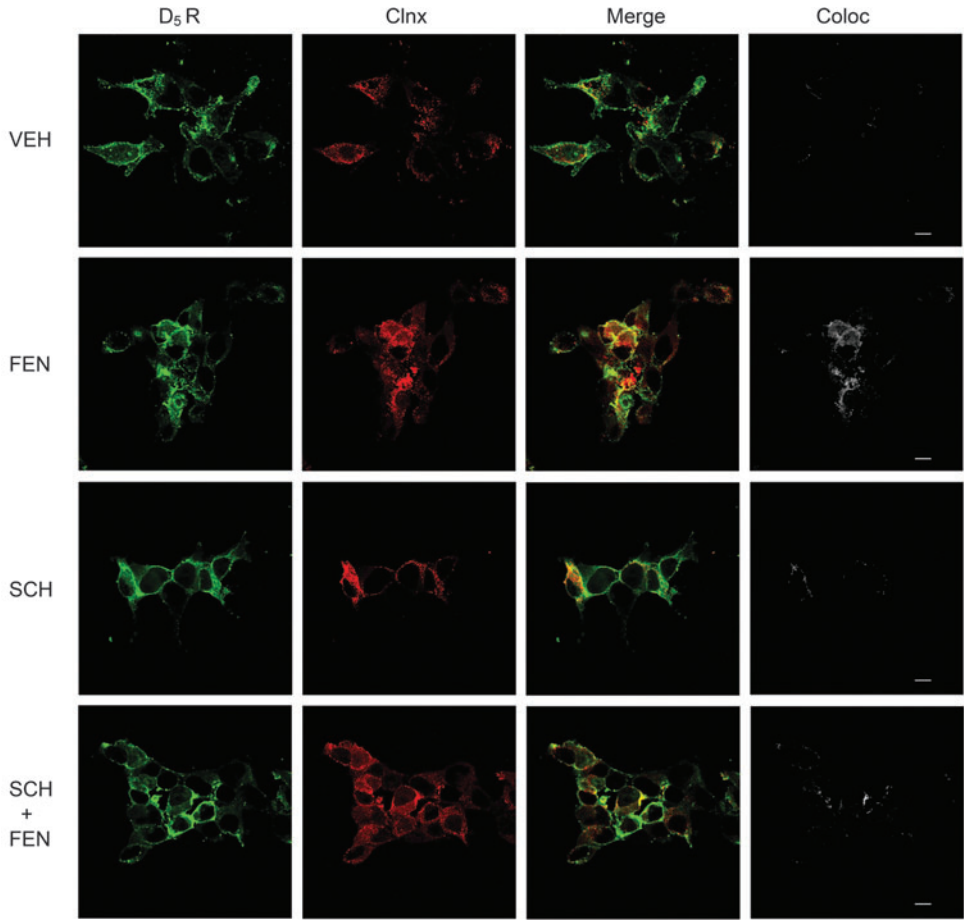

FIG. 4. The D_5R resides in the endoplasmic reticulum in D_5R-HEK293 cells. Cells were treated with VEH or D_1R/D_5R agonist, FEN (25 n*M*, 12 h), in the absence or presence of the D_1R/D_5R antagonist, SCH (1 μM, 12 h), as indicated. The cells were then immunostained with anti-D_5R (*green*) and anti-calnexin (Clnx, *red*) antibodies. Clnx is an ER marker. Co-localization (*yellow*) of D_5R and Clnx was increased by FEN treatment that was blocked by SCH treatment, which by itself had no effect. $n = 3$/group. A panel of separate colocalization images in ''Coloc'' were generated as described in the Methods section. Scale bar, 10 μm. ER, endoplasmic reticulum.

silencing impaired the FEN-mediated reduction of the production of these proinflammatory cytokines (Fig. 7).

Similar results were observed in hRPTCs, as siRNA-induced silencing of *PRDX4* increased IL-1β and TNF production and impaired the inhibitory effect of FEN on the production of these proinflammatory cytokines (Supplementary Fig. S4).

Immunoblotting further confirmed that the siRNA-induced *PDRX4* knockdown increased TNF protein expression in D_5R-HEK293 cells; the increase in TNF protein expression was attenuated by tempol (Supplementary Fig. S5), a redox cycling nitroxide that metabolizes ROS (Wilcox, 2010), indicating that the deficiency of PRDX4 increased ROS production that mediated the increase in proinflammatory cytokines.

ER-resident caspase-12 is increased by PRDX4 silencing

Caspases are cysteine proteases that play important roles in the regulation of inflammation (Bolívar et al, 2019). Since caspase-12 is the only caspase that resides in the ER (García de la Cadena and Massieu, 2016), we evaluated the effect of PRDX4 on the production of caspase-12.

In VEH-treated D_5R-HEK293 cells and hRPTCs, siRNA silencing of *PRDX4* increased the production of caspase-12 from 100.0 ± 25.3% to 268.2 ± 28.1% ($n = 4$/group) (Fig. 8A) and 100 ± 12.9% to 318.3 ± 22.5% ($n = 4$/group) (Supplementary Fig. S6A), respectively. By contrast, FEN decreased the production of caspase-12 in scrambled siRNA- but not in the *PRDX4* siRNA-transfected cells (Fig. 8A and Supplementary Fig. S6A).

To determine further the effect of PRDX4 on procaspase-12 and cleaved caspase-12, the active form of caspase-12, we immunoblotted cell lysates from D_5R-HEK293 (Fig. 8B) and hRPTCs (Supplementary Fig. S6B) treated with increasing concentrations of FEN. Low concentrations of FEN (2.5 and 25 n*M*) decreased both procaspase-12 and cleaved caspase-12 proteins (Figs. 8B and Supplementary S6B).

PRDX4 protein expression is reduced in the kidney of Drd5$^{-/-}$ mice

Drd5$^{-/-}$ mice are hypertensive and in a state of oxidative stress (Hollon et al, 2002; Yang et al, 2006). In non-reducing condition, both dimeric (41.2% ± 4.5% vs.100.0% ± 5.9%, n = 4) and monomeric (35.5% ± 3.9% vs.100.0% ± 5.5%, n = 4/group) (Fig. 9A) forms of PRDX4 in renal cortices of *Drd5*$^{-/-}$ mice were decreased, relative to their *Drd5*$^{+/+}$, wild-type littermates. In reducing condition, only the monomeric form of PRDX4 was found, which was also decreased in renal cortices of *Drd5*$^{-/-}$ mice, relative to their *Drd5*$^{+/+}$, wild-type littermates (57.3% ± 3.7% vs.100.0% ± 5.8%, n = 4/group) (Fig. 9B). The reduced PRDX4 protein expression in *Drd5*$^{-/-}$ mice indicates a potential interaction *in vivo* between D_5R and PRDX4 in the regulation of ROS in the mouse kidney.

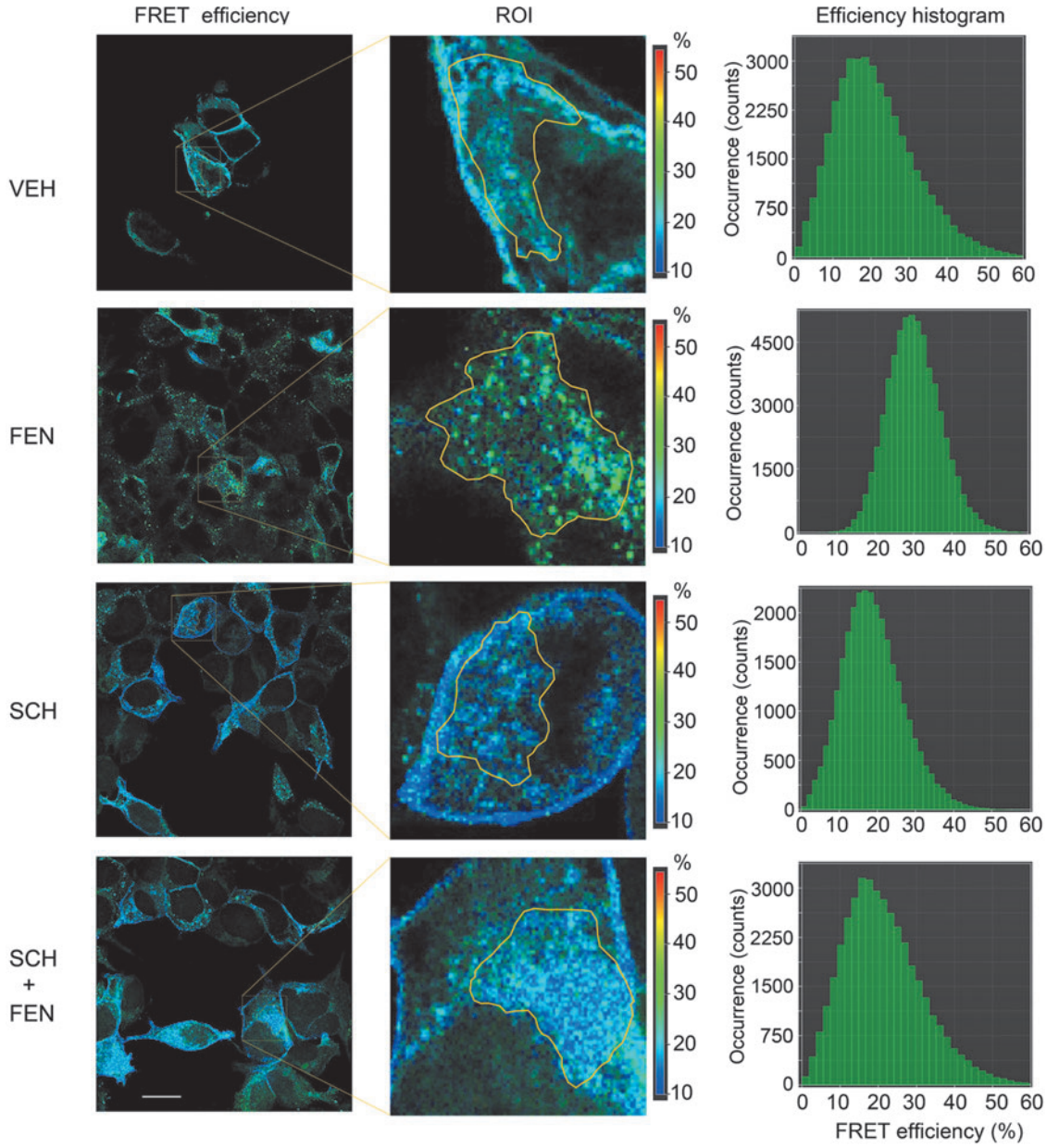

FIG. 5. FRET between D_5R and PRDX4 in D_5R-HEK293 cells. Alexa Fluor 488 conjugated with anti-D_5R (as FRET donor), and Alexa Fluor 555 conjugated with PRDX4 (as FRET acceptor) were used to determine the spatial proximity between the D_5R and PRDX4 by FLIM-based FRET analysis. ROI were drawn in the cytoplasm, presumably the ER area, from 10 to 15 cells of three to five random fields under the microscope. The representative FRET efficiency heatmap images, ROI, and FRET efficiency histogram are shown for each treatment. Scale bar (along the ROI) and the histogram (x-axis) show the values of FRET efficiency (%) from the ROI of representative images. Experiments were independently performed two to three times with similar results. ROI, regions of interest; FRET, fluorescence (Förster) resonance energy transfer.

Proinflammatory cytokine protein expression is increased in the kidney of $Drd5^{-/-}$ mice

We further determined the renal protein expression of IL-1β, TNF, and caspase-12 in $Drd5^{-/-}$ mice. As shown in Figure 10, protein expression of IL-1β (175.3% ± 19.8% vs. 100.0% ± 10.8%, n = 4) (Fig. 10A) and TNF (148.5% ± 9.8% vs. 100.0% ± 10.0%, n = 4/group) (Fig. 10B) was increased in renal cortices of $Drd5^{-/-}$ mice, relative to their $Drd5^{+/+}$ wild-type littermates.

The protein expression of both pro-caspase-12 (277.6% ± 42.8% vs.100.0% ± 31.8%, n = 4) and cleaved caspase-12 (263.1% ± 32.8% vs.100.0 ± 31.0%, n = 4) was also increased in the renal cortices of $Drd5^{-/-}$ mice, relative to their $Drd5^{+/+}$ wild-type littermates (Fig. 10C).

Discussion

Oxidative stress, the imbalance between the production and scavenging of ROS, and inflammation are implicated in

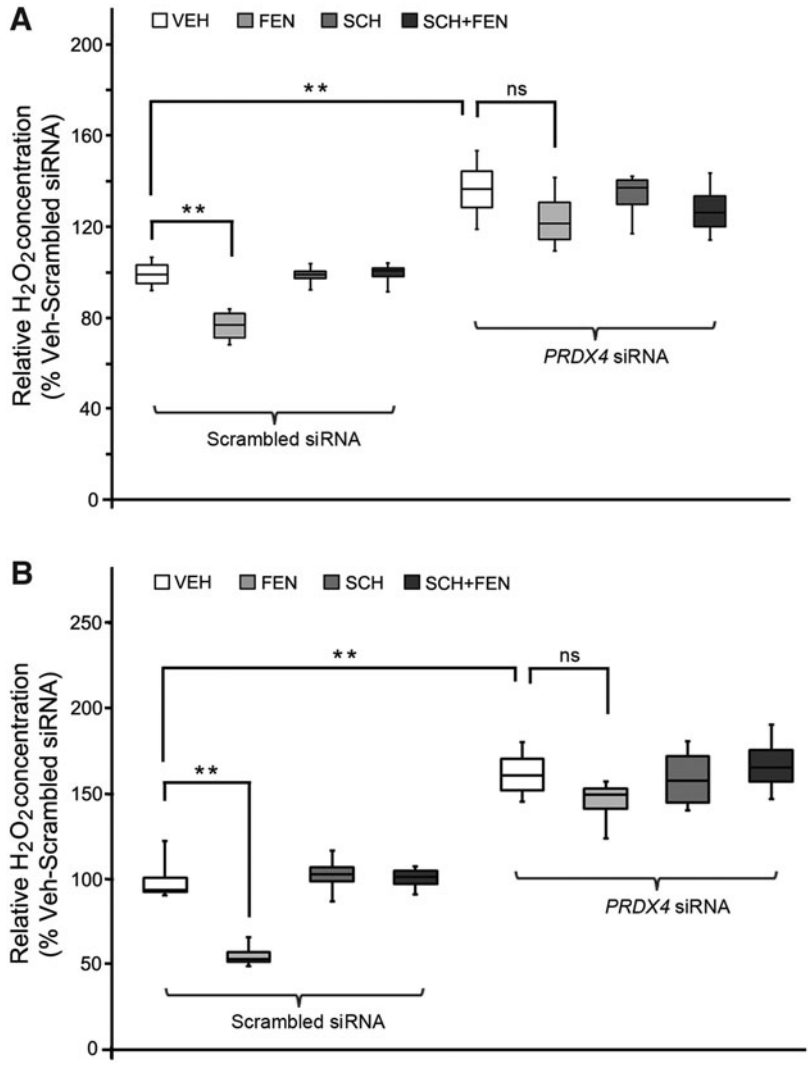

FIG. 6. Hydrogen peroxide production in *PRDX4*-silenced D_5R-HEK293 cells and hRPTCs. D_5R-HEK293 cells **(A)** and hRPTCs **(B)** were transfected with *PRDX4*-scrambled or -specific siRNA for 36 h and then treated with VEH or D_1R/D_5R agonist, FEN (25 n*M*, 12 h), in the absence or presence of the D_1R/D_5R antagonist, SCH (1 μM, 12 h), as indicated. The culture media were collected, and hydrogen peroxide concentration was measured by Amplex Red. The fluorescence intensity was measured in a microplate reader. $n = 4$/group, ns, not significant; $^{**}p < 0.01$; two-way ANOVA, Newman–Keuls test. hRPTC, human renal proximal tubule cell.

many pathological conditions, such as chronic inflammatory diseases, including hypertension, and acute kidney and chronic kidney diseases, among others (Bonventre and Zuk, 2004; Harris and DeNicola, 2020; Konno et al, 2021; Nano et al, 2022; Qaddumi and Jose, 2021; Xiao and Harrison, 2020; Zeng et al, 2009). The results of this study could open a new target of PRDX4 to prevent the initiation and progression of hypertension and acute and chronic kidney diseases and their complications.

Dopamine, through D_1-like (D_1R and D_5R) and D_2-like (D_2R, D_3R and D_4R) receptors, decreases ROS production in the kidneys of humans and animals (Lee et al, 2021; Lu et al, 2013; Qaddumi and Jose, 2021; Stoelting et al, 2009; Tayebati et al, 2011; Yang et al, 2006; Yang et al, 2015; Yu et al, 2014), but may be different in other cells (Acquier et al, 2013), especially in neurons (Qaddumi and Jose, 2021). The D_5R negatively regulates ROS production, in part, through the inhibition of NADPH oxidase and mitochondria-derived ROS (Lee et al, 2021; Yang et al, 2006) and in part, through the increase of enzymatic and non-enzymatic antioxidant scavengers, including heme oxygenase-1 (Lu et al, 2013), paraoxonase 2 (Yang et al, 2015), and thioredoxin (Wang et al, 2019). The current study demonstrates that FEN, a D_5R agonist (in the absence of D_1R), decreased ROS (hydrogen peroxide) production and inflammation through the ER-resident PRDX4 in the kidney.

The ER is an essential organelle for the proper folding and posttranslational modification of newly synthesized proteins (McLaughlin and Vandenbroeck, 2011). The GPCRs are synthesized, assembled, folded, and mature in the ER (Magalhaes et al, 2012). Therefore, ER-resident proteins could participate in the regulation of GPCR expression, signaling, and trafficking. Calnexin, a well-known ER chaperone protein, interacts with D_1R and D_2R and regulates their glycosylation and cell surface expression (Free et al, 2007).

Cornichon Family AMPA Receptor Auxiliary Protein 4 (CNIH4), an ER protein, promotes β_2-adrenergic receptor retention, leading to its proteasomal degradation (Sauvageau et al, 2014). The dopamine receptor-interacting protein 78, another ER resident protein, regulates the residence of D_1R in the ER, as well as its ligand binding and glycosylation (Bermak et al, 2001). In our current study, the activation of D_5R increased the protein expression of PRDX4, an ER resident PRDX.

Whether or not D_5R increases PRDX4 protein expression through an increase in transcription/translation or a decrease

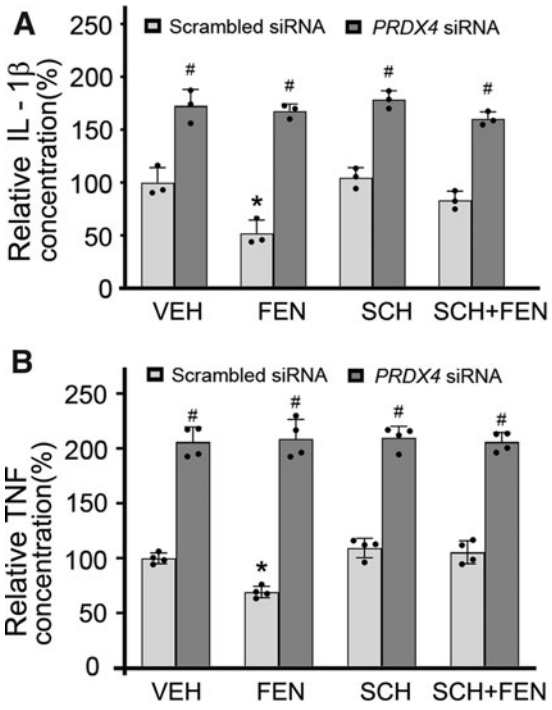

FIG. 7. Productions of IL-1β (A) and TNF (B) are increased in *PRDX4*-silenced D_5R-HEK293 cells. D_5R-HEK293 cells were transfected with *PRDX4*-scrambled or -specific siRNA for 36 h and then treated with VEH or the D_1R/D_5R agonist, FEN (25 n*M*, 12 h), in the absence or presence of the D_1R/D_5R antagonist, SCH (1 μM, 12 h), as indicated. The concentrations of IL-1β **(A)** and TNF **(B)** in the culture media were measured by ELISA. $n = 3$ or 4/group, $^{*}p < 0.05$ *versus* VEH, $^{\#}p < 0.05$ *versus* scrambled siRNA, two-way ANOVA, Newman–Keuls test. IL-1β, interleukin-1β; TNF, tumor necrosis factor.

in its degradation and/or apoptosis remains to be determined. Nonetheless, the increase in the expression of PRDX4 in non-LRs on D_5R activation could play a vital role in its inhibition of production of ROS (*e.g.,* hydrogen peroxide), proinflammatory cytokines, and caspase-12 production.

Oxidative protein folding is one of the major effects of ROS in the ER (Ramming et al, 2015). In our current study, the stimulation of D_5R increased its localization in the ER and interaction with PRDX4. However, short-term (FEN 25 nM, 15 min) treatment did not increase the redistribution of D_5R into the ER as determined by co-localization of D_5R with either PRDX4 or calnexin (not shown). The increase of D_5R colocalization with PRDX4 in ER in the condition of this study (FEN 25 nM, 12 h) was most likely caused by the increase in the PRDX4 production or maturation or the decrease in degradation, including ER-associated degradation. However, the possibility of redistribution could not be excluded, which needs further investigation.

The siRNA-mediated silencing of *PRDX4* increased hydrogen peroxide production and impaired the inhibitory effect of D_5R on hydrogen peroxide production in D_5R-HEK293 and hRPTCs. This is consistent with previous reports that *Prdx4* knockout mice have increased lipid and protein oxidation in spermatocytes (Iuchi et al, 2009) and overexpression of PRDX4, as in *Prdx4* transgenic mice, attenuated oxidative stress, inflammation, and cytokine release in different organs (Yamada and Guo, 2018). Of interest is that germline deletion of *Prdx2* aggravates the oxidative stress and increased blood pressure of spontaneously hypertensive rats (Mahal et al, 2019).

The ER is susceptible to oxidative stress because it has low levels of antioxidants; oxidative stress induces ER stress, and vice versa (Cao and Kaufman, 2014). Prolonged oxidative and ER stresses contribute to the inflammatory cascade, resulting in the activation of immune cells and the production of proinflammatory cytokines in the kidney (Xiong et al, 2021). Macrophages are the main inflammatory cells infiltrating the kidney with chronic inflammatory disease (Lee et al, 2020). Renal tubule cells can also initiate the inflammatory response.

In hRPTCs, the gene and protein expressions of IL-1β, caspase-1, and toll-like receptor 4 are increased by uric acid (Xiao et al, 2015), an ROS inducer (Oğuz et al, 2017). In the human kidney-2 cell, a proximal tubule cell line derived from a normal human kidney, IL-1β levels are increased by monosodium urate (Hong et al, 2015). In HEK293 cells, proinflammatory cytokines trigger the NF-κB pathway, which is attenuated by ROS inhibition (Shi et al, 2020). In our current study, proinflammatory IL-1β and TNF levels were decreased by D_5R activation but increased by the silencing of *PRDX4* in D_5R-HEK293 and hRPTCs. This may be through the NF-κB/NLRP3 inflammasome pathway because IL-1β is the major cytokine released by the activation of NLRP3 inflammasomes (Lee et al, 2020).

Persistent inflammation alongside severe or prolonged oxidative and ER stress induces the apoptosis pathway (Gorman et al, 2012). Caspase-12, located in the cytoplasmic side of the ER, is an ER stress-associated inflammatory caspase that regulates the canonical ER stress-mediated apoptotic pathways, which include PERK pathway-induced CHOP activation and IRE1α pathway-induced JNK and caspase-12 activation (Rong et al, 2015).

Our data showed that D_5R activation decreased caspase-12 production, which was impaired by *PRDX4* silencing. The fact that D_5R stimulation decreased both pro- and cleaved-caspase-12 suggests that the D_5R activates upstream of caspase-12 posttranslational cleavage, possibly via the NF-κB like pathway, which warrants further investigation. The apparent role of PRDX4 in the D_5R-mediated decrease in hydrogen peroxide production and inflammation is important, indicating that D_5R may play important roles in a wide range of chronic inflammatory and oxidative stress disorders.

The decrease in the production of caspase-12 was dependent on D_5R-mediated stimulation of PRDX4. This indicates that the D_5R could play a critical role in ER-dependent apoptosis. Apoptosis contributes to the development and pathogenesis of diverse disorders (Singh et al, 2019b); apoptosis is increased in the kidney, ventricular cardiomyocytes, and vascular smooth muscle cells from spontaneously hypertensive rats and mice (Hamet et al, 1995). Apoptosis and NF-κB activation are simultaneously induced in the renal tubulointerstitium in angiotensin II-infusion-mediated hypertension (Quiroz et al, 2003).

The D_5R antagonizes the effect of angiotensin II, by decreasing the expression of the angiotensin II type 1 receptor (Gildea et al, 2008; Li et al, 2008). Therefore, it will be necessary to determine the mechanisms by which D_5R inhibits apoptosis in the ER in RPTCs.

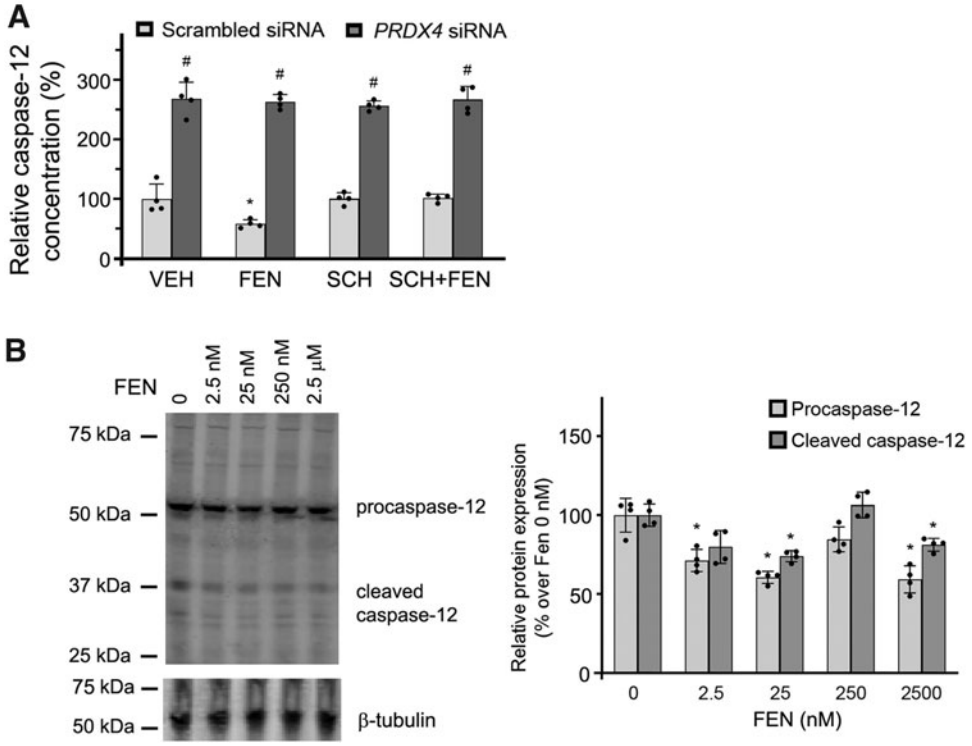

FIG. 8. Caspase-12 expression is inhibited by FEN treatment in D_5R-HEK293 cells. (A) D_5R-HEK293 cells were transfected with *PRDX4*-scrambled or -specific siRNA for 36 h and then treated with VEH or D_1R/D_5R agonist, FEN (25 n*M*, 12 h), in the absence or presence of D_1R/D_5R antagonist, SCH (1 μM, 12 h). The concentrations of caspase-12 in the culture medium were measured by ELISA. $n = 4$/group, $^*p < 0.05$ *versus* VEH, $^{\#}p < 0.05$ *versus* scrambled siRNA, two-way ANOVA, Newman–Keuls test. **(B)** The D_5R-HEK293 cells were treated with increasing concentrations of FEN (12 h), as indicated. The cell lysates were subjected to 10% SDS-PAGE and immunoblotted with anti-caspase12 antibody. β-tubulin was used as loading control. $n = 4$/group, $^*p < 0.05$ *versus* VEH-treated (0) group, one-way ANOVA, Newman–Keuls test.

In summary, stimulation of the D_5R, independent of the D_1R, increased PRDX4 protein expression, mainly in the non-LR microdomain in D_5R-HEK293 cells. Stimulation of D_5R increased its residence in the ER and its interaction with PRDX4 in D_5R-HEK293 and hRPTCs. The production of hydrogen peroxide and proinflammatory cytokines was increased by *PRDX4* silencing, which impaired the inhibitory effect of D_1R/D_5R stimulation on hydrogen peroxide and proinflammatory cytokine production. The increase in TNF with *PRDX4* silencing was attenuated by the antioxidant, tempol, indicating the importance of ROS (hydrogen peroxide) in this process.

D_5R stimulation also attenuated caspase-12 production, implying its potential role in ER stress-associated apoptosis; this effect is probably *via* PRDX4 because siRNA silencing of *PRDX4* increased caspase-12 expression and prevented the inhibitory effect of D_5R stimulation. Furthermore, in *Drd5*$^{-/-}$ mice, which are in a state of oxidative stress, the renal cortical PRDX4 protein expression was decreased, relative to their normotensive wild-type littermates.

These results suggest that D_5R negatively regulates hydrogen peroxide production and inflammation through PRDX4 in the kidney. Thus, the D_5R maintains a normal redox balance by promoting antioxidant activity, mediated, in part, by PRDX4, heme oxygenase-1, paraoxonase 2, and thioredoxin, and by inhibiting pro-oxidant activities, mediated by NADPH oxidase and mitochondria.

Materials and Methods

Electronic laboratory notebook was not used. All animal experiments were performed under protocols approved by the Children's National Medical Center, University of Maryland School of Medicine, and George Washington University Animal Care and Use Committees. The usage of human renal proximal tubule cells was approved by the Institutional Review Board of University of Virginia (protocol code HSR# 13310, 8/24/23).

Antibodies and reagents

We used anti-D_5R antibodies, which have been validated in *Drd5*$^{-/-}$ mice and studies involving hRPTCs and rat kidneys (Hollon et al, 2002; Lee et al, 2021; Wang et al, 2010; Yang et al, 2006). The anti-PRDX4 antibody was purchased from Abcam (Waltham, MA). The validation of PRDX4 antibody was performed by both the supplier (knockout cell lines generated *via* CRISPR-Cas9) and in our laboratory in *PRDX4*-specific siRNA-transfected D_5R-HEK293 cells (Supplementary Fig. S7A, C) and hRPTCs (Supplementary Fig. S7B, C).

Normal chicken IgY, anti-β-tubulin, and anti-α-actin antibodies were purchased from Sigma (St. Louis, MO); anti-calnexin antibody was purchased from ECM Biosciences (Versailles, KY); anti-TNF antibody was purchased from Cell Signaling Technology (Danvers, MA), and anti-caspase-12 and normal rabbit Ig G were purchased from Santa Cruz

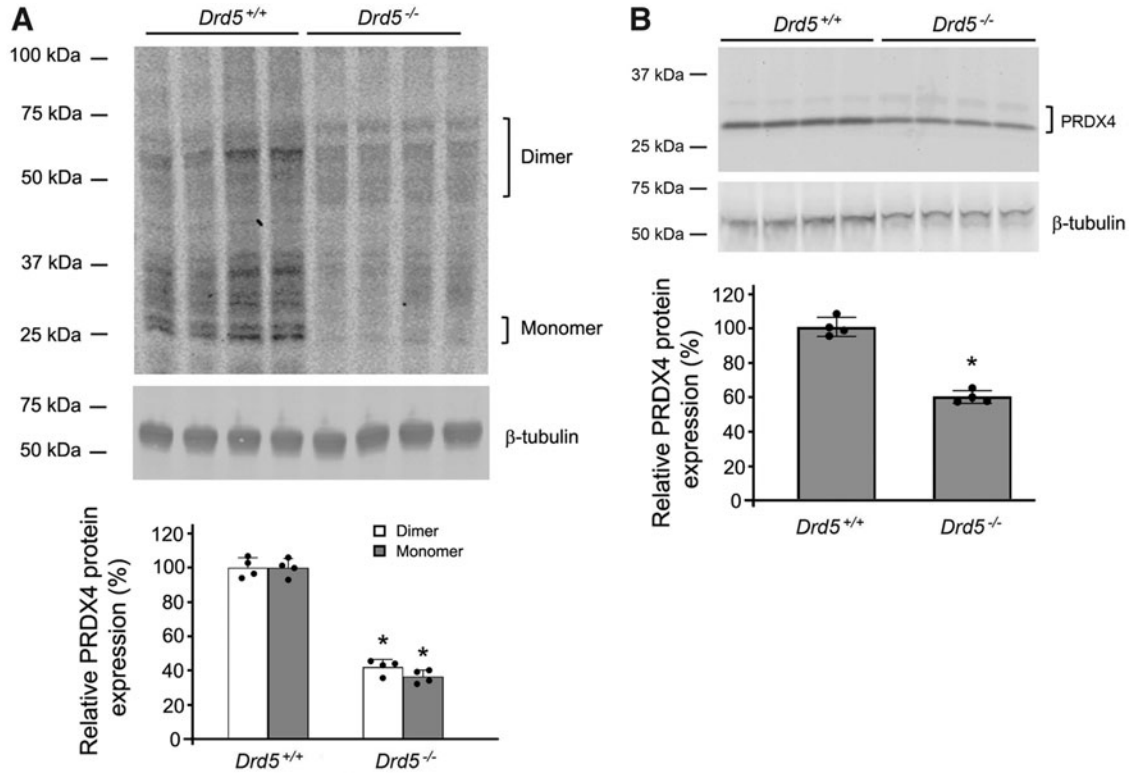

FIG. 9. PRDX4 protein expression in kidney cortices from *Drd5*$^{-/-}$ and their wild-type littermates. Kidney cortices from *Drd5*$^{-/-}$ mice and their wild-type (*Drd5*$^{+/+}$) littermates were prepared in non-reducing **(A)** or reducing (**B**, 5% 2- mercaptoethanol) Laemmli buffer and subjected to10% SDS-PAGE. β-tubulin was used for loading control. PRDX4 protein expression, determined by western blotting, was decreased in kidney cortices of *Drd5*$^{-/-}$ mice, relative to *Drd5*$^{+/+}$ wild-type littermates. $n = 4$/group, $^{*}p < 0.05$, Student's t test.

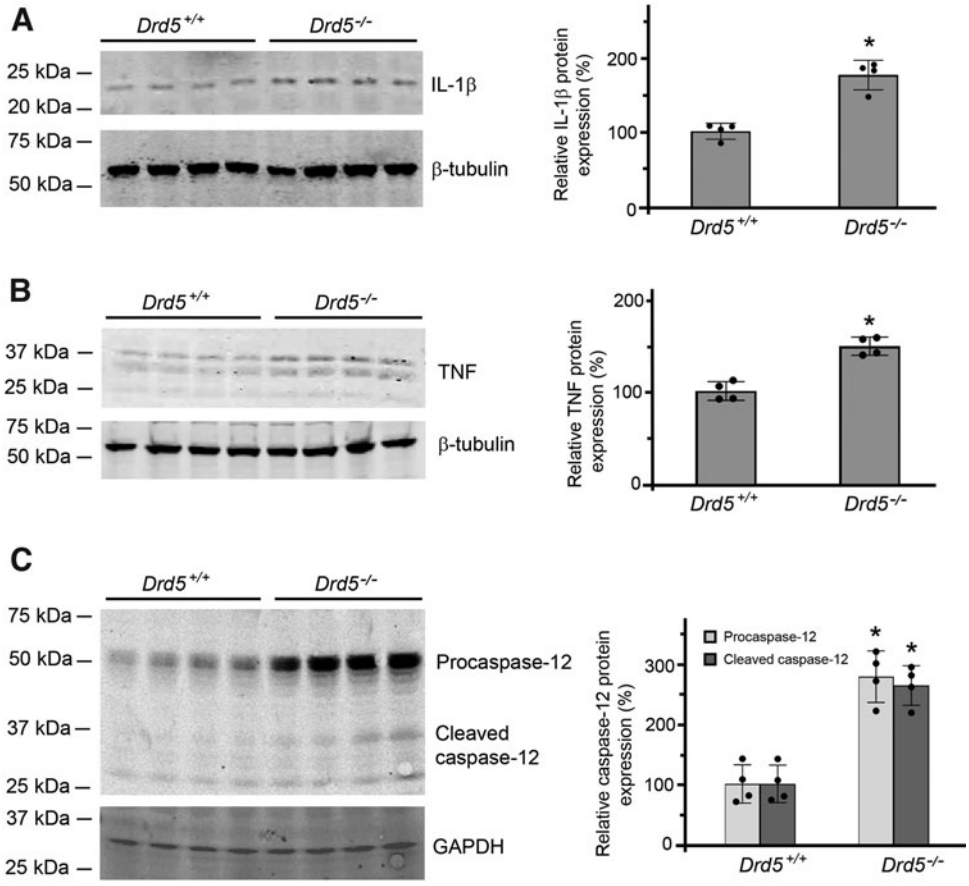

FIG. 10. Protein expression of interleukin-1β (A), tumor necrosis factor (B), and caspase-12 (C) in renal cortices from *Drd5*$^{-/-}$ and their wild-type littermates. Kidney cortices from *Drd5*$^{-/-}$ mice and their wild-type (*Drd5*$^{+/+}$) littermates were prepared in Laemmli buffer and subjected to 10% SDS-PAGE. β-tubulin or GAPDH was used for loading control. $n = 4$/group, $^{*}p < 0.05$, Student's t test.

Biotechnology (Santa Cruz, CA). Culture media and fetal bovine serum (FBS) were purchased from Invitrogen (Gaithersburg, MD). Fenoldopam (FEN), SCH 39166 (SCH), and tempol were purchased from Tocris (Minneapolis, MN); methyl-β-cyclodextrin (M-β-CD) and other reagents were purchased from Sigma.

Cell culture, siRNA, and transfection

HEK293 cells expressing D_5R (D_5R-HEK293), and hRPTCs were cultured, as previously described (Li et al, 2008; Yu et al, 2014). The empty vector-transfected HEK293 and D_5R-HEK293 cells were maintained in culture with 10 μg/mL blasticidin. The stable protein expression of D_5R in D_5R-HEK293 cells was confirmed before the actual experiments were performed (Lee et al, 2021; Lu et al, 2013; Yu et al, 2014).

hRPTCs were verified of their RPT origin, by staining with antibody against γ-glutamyl transpeptidase and expression of NHE3 (Gildea et al, 2014; Gildea et al, 2008; Li et al, 2008; Sanada et al, 1999; Yu et al, 2014). The cells were cultured in a 1:1 mixture of Dulbecco's modified Eagle's medium and Ham's F-12 medium, supplemented with 5% FBS, selenium (5 ng/mL), insulin (5 μg/mL), transferrin (5 μg/mL), hydrocortisone (36 ng/mL), triiodothyronine (4 pg/mL), and epidermal growth factor (10 ng/mL).

PRDX4-scrambled and -specific siRNA (Qiagen) were transfected into hRPTCs and D_5R-HEK293 cells grown in 12- or 24-well plates using Lipofectamine 2000 transfection reagents (Invitrogen), according to the manufacturer's instructions and our published procedure (Lee et al, 2021; Yang et al, 2015). The efficiency of siRNA in silencing *PRDX4* was determined by both immunoblotting (Supplementary Fig. S7A, B) and quantitative real-time PCR (Supplementary Fig. S7C).

Western blotting

The samples (D_5R-HEK293 cells, hRPTCs, and kidney cortices) were lysed in 1x RIPA lysis buffer (Millipore, Billerica, MA), containing protease and phosphatase inhibitor cocktail (Thermo Fisher Scientific, Rockford, IL), and they were adjusted to the same protein concentration. The proteins were separated by sodium dodecyl sulfate-polyacrylamide gel electrophoresis (SDS-PAGE), transferred onto nitrocellulose membranes, and then probed with primary antibodies and appropriately conjugated secondary antibodies. The images were visualized by a LiCor Odyssey Imaging system.

Subcellular fractionation

To obtain LRs and non-LRs, HEK293 cells were subjected to sucrose gradient centrifugation, using a detergent-free protocol, as previously described (Li et al, 2009; Yang et al, 2015; Yu et al, 2014). Briefly, the cell pellets were lysed in 1.5 mL of 500 m*M* sodium carbonate (pH 11) and homogenized in clear ultracentrifuge tubes. Equal amounts of homogenates were diluted 1:2 with 80% sucrose and overlaid with 5–35% sucrose, as a discontinuous sucrose gradient and subjected to centrifugation at 160,000 *g* for 16 h at 4°C.

After centrifugation, twelve 1-mL fractions were collected, and a light-scattering band was confined to the 5–35% sucrose interface; fractions 1–6 were considered as LRs, whereas fractions 7–12 were considered as non-LRs (Li et al, 2009; Yang et al, 2015; Yu et al, 2014). The fractionated proteins were mixed with reducing Laemmli buffer, containing 5% 2-mercaptoethanol, boiled, and subjected to SDS-PAGE. The transfer of the protein (from the gel onto the cellulose membrane) was performed using a constant current and duration to obtain the same transfer efficiency from the gel.

Co-immunoprecipitation

Co-immunoprecipitation was performed using a Dynabeads kit (Thermo Fisher Scientific), following the manufacturer's instruction, and as previously described (Li et al, 2010). Briefly, D_5R-HEK293 and hRPTCs were treated with VEH, D_1R/D_5R agonist, FEN (25 n*M*, 12 h) in the absence or presence of 1 μ*M*, 12 h, D_1R/D_5R antagonist, SCH (Tice et al, 1994). The cells were harvested, and the cell pellets were lysed in a lysis buffer (20 m*M* Tris·HCl, pH 8.0/1 m*M* ethylenediaminetetraacetic acid/1 m*M* NaN3/2 m*M* dithiothreitol/0.25 *M* sucrose), with 0.2 m*M* phenylmethylsulfonyl fluoride, and protease and phosphatase inhibitor cocktail.

Five μg of anti-PRDX4 or anti-D_5R antibody were conjugated with Dynabeads in 0.5 mL of slurry. The cell lysates were then incubated with the conjugated anti-D_5R or anti-PRDX4 antibodies at 4°C for 4 h, followed by proper washing. Controls were normal rabbit IgG and chicken IgY. Proteins bound to the beads were eluted in 60 μL of loading buffer at 65°C for 15 min, separated by 10% SDS-PAGE, and transferred onto a nitrocellulose membrane for incubation with the detecting antibody, followed by the appropriate secondary antibody, before visualization with a LiCor Odyssey Imaging system.

Confocal fluorescence microscopy and colocalization analysis

D_5R-HEK293 or hRPTCs were fixed with 4% paraformaldehyde in phosphate-buffered saline (PBS) for 20 min at room temperature. After washing with PBS, the fixed cells on coverslips were incubated with primary anti-PRDX4, anti-D_5R, or anti-calnexin antibodies overnight at 4°C. The coverslips were then incubated with the proper Alexa Fluor-488 and -555 secondary antibodies for 2 h at 4°C. The coverslips were mounted in an antifade mounting medium (Vectashield, Burlingame, CA) and sealed onto glass slides. The samples were imaged with a Zeiss laser scanning microscope (LSM) 710 confocal microscope system equipped with a Plan-Apochromat 63×/1.40 NA oil-immersion objective.

Colocalization of two labels was analyzed using the ''Colocalization'' module of IMARIS 9.8 version (Bitplane AG, Saint Paul, MN). The confocal images for the two labels, generated by the ZEISS LSM710 confocal microscope, were opened with IMARIS and converted into an Imaris file. Interactive thresholding was initially used to estimate the thresholds for each label. Then, threshold values were manually tuned to eliminate the background pixels. Once the individual label thresholds were set, they were used to define colocalization, and the colocalization channel was generated following the procedure of the program.

FLIM-FRET analysis

The FLIM-FRET analysis was performed, as previously described (Li et al, 2010) with modification. The fluorophore

pairs used for FLIM-FRET analysis were Alexa Fluor 488 (as FRET donor) conjugated with anti-D_5R antibody and Alexa Fluor 555 conjugated with anti-PRDX4 antibody (as FRET acceptor). Time-domain FLIM-based FRET was performed with a Leica TCS SP8 microscope system upgraded to FALCON, equipped with a tunable ultrafast (80 megahertz) pulsed (120 fs) laser (Coherent), HyD SMD detectors (time-correlated single photon counting and time-gated system), and an HC PL APO CS2 100×/1.44 OIL objective (Leica Microsystems).

The samples were excited with an 800 nm laser, 3.5 w, tube current, 100 frame repetitions, with 500–550 nm detection window and processed using the built-in FLIM/FCS module. A lower intensity threshold was set to 50 photons for all image analyses. The lifetime values and FRET efficiency images were generated with the built-in Leica Application Suite FLIM/FCS (Leica Wetzlar).

Hydrogen peroxide production

Hydrogen peroxide production from cell lysates was measured by Amplex Red (Invitrogen, Eugene, OR), in the presence of exogenous superoxide dismutase (40 U/mL) and horseradish peroxidase (10 U/mL), as described (Lee et al, 2021), with modification. Briefly, D_5R-HEK293 and hRPTCs were grown in 24-well plates. The cells were transfected with *PRDX4*-scrambled or -specific siRNA for 36 h when the cells were about 75% confluent.

Then, the cells were centrifuged, and 50 μL supernatants from each well were incubated with 50 μL freshly prepared Amplex Red (100 μM) and horseradish peroxidase (0.2 U/mL) for 15 min at room temperature. Resorufin, the fluorescent product, was measured in triplicate in a fluorescence 96-well plate reader at an excitation wavelength of 530 nm and an emission wavelength of 590 nm.

Enzyme-linked immunosorbent assay

The concentrations of IL-1β (Cayman Chemical, Ann Arbor, MI), TNF (Cayman Chemical), and caspase-12 (Antibodies-Online, Inc., Limerick, PA) were measured using enzyme-linked immunosorbent assay kits, according to the manufacturers' instructions. Briefly, D_5R-HEK293 and hRPTCs were seeded in 12-well plates; the cells were transfected with *PRDX4* -scrambled or -specific siRNA when the cells were about 75% confluent. After 36 h, FEN (25 nM) or VEH was added in the presence or absence of SCH (1 μM, 30 min earlier than FEN) for 12 h. The supernatants from the samples were collected by centrifugation, and their absorbances were read in 96-well plates at 410 nm, for IL-1β and TNFα, and 450 nm, for caspase-12.

Generation of Drd5$^{-/-}$ mice

The generation of *Drd5*$^{-/-}$ mice has been reported (Hollon et al, 2002; Lee et al, 2021; Li et al, 2008; Yang et al, 2006); *Drd5*$^{-/-}$ mice are hypertensive and in a state of oxidative stress (Lee et al, 2021; Lu et al, 2013; Yang et al, 2006). F6 generation *Drd5*$^{-/-}$ mice on C57Bl/6 (>98% congenic) background and sex-matched, wild-type littermates were used in this study. The kidneys were collected, and their cortices were processed for immunoblotting (Hollon et al, 2002; Lee et al, 2021; Li et al, 2008; Yang et al, 2006).

Statistical analysis

Sample sizes were determined by power calculation with the type I and type II significance levels at 0.05 and power to 0.8. Results are expressed as mean ± standard deviation. Significant differences among groups ($n > 2$) were determined by one-way factorial ANOVA, Newman–Keuls test, and between two groups by Student's t test. $p < 0.05$ was considered statistically significant (SigmaStat 3.0, SPSS, Inc., Chicago, IL).

Author Disclosure Statement

All the authors declare no competing interests.

Authors' Contribution

H.L. and P.A.J. conceived and designed the experiments. B.A., S.Y., P.Y., L.D.A., and H.L. performed the experiments. B.A., P.Y., P.V.C., I.A., C.Z., R.A.F., L.D.A., P.A.J., and H.L. interpreted the experimental results. H.L. drafted the manuscript; all authors edited and revised the manuscript. P.A.J. approved the final manuscript.

Data Availability

The data are available upon reasonable request.

Funding Information

This study was supported, in part, by grants from National Institutes of Health R01DK119652, R37HL023081, R01DK039308, and P01HL074940. The authors appreciate Dr. Anastas Popratiloff's imaging assistance at the George Washington University Nanofabrication and Imaging Center (GWNIC).

Supplementary Material

Supplementary Figure S1
Supplementary Figure S2
Supplementary Figure S3
Supplementary Figure S4
Supplementary Figure S5
Supplementary Figure S6
Supplementary Figure S7

References

Abbasi A, Corpeleijn E, Postmus D, et al. Peroxiredoxin 4, a novel circulating biomarker for oxidative stress and the risk of incident cardiovascular disease and all-cause mortality. J Am Heart Assoc 2012;1(5):e002956; doi: 10.1161/JAHA.112.002956

Acquier AB, Mori Sequeiros García M, Gorostizaga AB, et al. Reactive oxygen species mediate dopamine-induced signaling in renal proximal tubule cells. FEBS Lett 2013;587(19): 3254–3260; doi: 10.1016/j.febslet.2013.08.020

Beaulieu JM, Gainetdinov RR. The physiology, signaling, and pharmacology of dopamine receptors. Pharmocol Rev 2011; 63(1):182–217; doi: 10.1124/pr.110.002642

Bermak JC, Li M, Bullock C, et al. Regulation of transport of the dopamine D1 receptor by a new membrane-associated ER protein. Nat Cell Biol 2001;3(5):492–498; doi: 10.1038/35074561

Bolduc J, Koruza K, Luo T, et al. Peroxiredoxins wear many hats: Factors that fashion their peroxide sensing personalities. Redox Biol 2021;42:101959; doi: 10.1016/j.redox.2021.101959

Bolívar BE, Vogel TP, Bouchier-Hayes L. Inflammatory caspase regulation: Maintaining balance between inflammation and cell death in health and disease. FEBS J 2019;286(14): 2628–2644; doi: 10.1111/febs.14926

Bonventre JV, Zuk A. Ischemic acute renal failure: An inflammatory disease? Kidney Int 2004;66(2):480–485; doi: 10.1111/j.1523-1755.2004.761_2.x

Cao SS, Kaufman RJ. Endoplasmic reticulum stress and oxidative stress in cell fate decision and human disease. Antioxid Redox Signal 2014;21(3):396–413; doi: 10.1089/ars.2014.5851

Castro B, Citterico M, Kimura S, et al. Stress-induced reactive oxygen species compartmentalization, perception and signalling. Nat Plants 2021;7(4):403–412; doi: 10.1038/s41477-021-00887-0

Crul T, Maléth J. Endoplasmic reticulum-plasma membrane contact sites as an organizing principle for compartmentalized calcium and cAMP signaling. Int J Mol Sci 2021;22(9):4703; doi: 10.3390/ijms22094703

Cuevas S, Asico LD, Jose PA, et al. Renal hydrogen peroxide production prevents salt-sensitive hypertension. J Am Heart Assoc 2020;9(1):e013818; doi: 10.1161/JAHA.119.013818

Elko EA, Manuel AM, White S, et al. Oxidation of peroxiredoxin-4 induces oligomerization and promotes interaction with proteins governing protein folding and endoplasmic reticulum stress. J Biol Chem 2021;296:100665; doi: 10.1016/j.jbc.2021.100665

Free RB, Hazelwood LA, Cabrera DM, et al. D1 and D2 dopamine receptor expression is regulated by direct interaction with the chaperone protein calnexin. J Biol Chem 2007; 282(29):21285–21300; doi: 10.1074/jbc.M701555200

García de la Cadena S, Massieu L. Caspases and their role in inflammation and ischemic neuronal death. Focus on caspase-12. Apoptosis 2016;21(7):763–777; doi: 10.1007/s10495-016-1247-0

Gildea JJ, Wang X, Jose PA, et al. Differential D1 and D5 receptor regulation and degradation of the angiotensin type 1 receptor. Hypertension 2008;51(2):360–366; doi: 10.1161/HYPERTENSIONAHA.107.100099

Gildea JJ, Shah IT, Van Sciver RE, et al. The cooperative roles of the dopamine receptors, D_1R and D_5R, on the regulation of renal sodium transport. Kidney Int 2014;86(1):118–126; doi: 10.1038/ki.2014.5

Gorman AM, Healy SJ, Jäger R, et al. Stress management at the ER: Regulators of ER stress-induced apoptosis. Pharmacol Ther 2012;134(3):306–316; doi: 10.1161/HYPERTENSIONAHA.107.100099

Hamet P, Richard L, Dam TV, et al. Apoptosis in target organs of hypertension. Hypertension 1995;26(4):642–648; doi: 10.1161/01.hyp.26.4.642

Harris IS, DeNicola GM. The complex interplay between antioxidants and ROS in cancer. Trends Cell Biol 2020;30(6): 440–451; doi: 10.1016/j.tcb.2020.03.002

Hollon TR, Bek MJ, Lachowicz JE, et al. Mice lacking D5 dopamine receptors have increased sympathetic tone and are hypertensive. J Neurosci 2002;22(24):10801–10810; doi: 10.1523/JNEUROSCI.22-24-10801.2002

Hong W, Hu S, Zou J, et al. Peroxisome proliferator-activated receptor γ prevents the production of NOD-like receptor family, pyrin domain containing 3 inflammasome and interleukin 1β in HK-2 renal tubular epithelial cells stimulated by monosodium urate crystals. Mol Med Rep 2015;12(24):6221–6226; doi: 10.3892/mmr.2015.4145

Iuchi Y, Okada F, Tsunoda S, et al. Peroxiredoxin 4 knockout results in elevated spermatogenic cell death via oxidative stress. Biochem J 2009;419(1):149–158; doi: 10.1042/BJ20081526

Kakihana T, Nagata K, Sitia R. Peroxides and peroxidases in the endoplasmic reticulum: Integrating redox homeostasis and oxidative folding. Antioxid Redox Signal 2012;16(8): 763–771; doi: 10.1089/ars.2011.4238

Konno T, Melo EP, Chambers JE, et al. Intracellular sources of ROS/H_2O_2 in health and neurodegeneration: Spotlight on endoplasmic reticulum. Cells 2021;10(2):233; doi: 10.3390/cells10020233

Lee H, Fessler MB, Qu P, et al. Macrophage polarization in innate immune responses contributing to pathogenesis of chronic kidney disease. BMC Nephrol 2020;21(1):270; doi: 10.1186/s12882-020-01921-7

Lee H, Jiang X, Perwaiz I, et al. Dopamine D5 receptor-mediated decreases in mitochondrial reactive oxygen species production are cAMP and autophagy dependent. Hypertens Res 2021;44(6):628–641; doi: 10.1038/s41440-021-00646-w

Li H, Armando I, Yu P, et al. Dopamine 5 receptor mediates Ang II type 1 receptor degradation via a ubiquitin-proteasome pathway in mice and human cells. J Clin Invest 2008;118(6): 2180–2189; doi: 10.1172/JCI33637

Li H, Han W, Villar VA, et al. D1-like receptors regulate NADPH oxidase activity and subunit expression in lipid raft microdomains of renal proximal tubule cells. Hypertension 2009;53(6):1054–1061; doi: 10.1161/HYPERTENSIONAHA.108.120642

Li H, Yu P, Sun Y, et al. Actin cytoskeleton-dependent Rab GTPase-regulated angiotensin type I receptor lysosomal degradation studied by fluorescence lifetime imaging microscopy. J Bio Optics 2010;15(5):056003; doi: 10.1117/1.3484751

Lipinski S, Pfeuffer S, Arnold P, et al. Prdx4 limits caspase-1 activation and restricts inflammasome-mediated signaling by extracellular vesicles. EMBO J 2019;38(20):e101266; doi: 10.15252/embj.2018101266

Lu Q, Yang Y, Villar VA, et al. D5 dopamine receptor decreases NADPH oxidase, reactive oxygen species and blood pressure via heme oxygenase-1. Hypertens Res 2013; 36(8):684–690; doi: 10.1038/hr.2013.9

Magalhaes AC, Dunn H, Ferguson SS. Regulation of GPCR activity, trafficking and localization by GPCR-interacting proteins. Br J Pharmacol 2012;165(6):1717–1736; doi: 10.1111/j.1476-5381.2011.01552.x

Mahal Z, Fujikawa K, Matsuo H, et al. Effects of the Prdx2 depletion on blood pressure and life span in spontaneously hypertensive rats. Hypertens Res 2019;42(5):610–617; doi: 10.1038/s41440-019-0207-9

Martinez VJ, Asico LD, Jose PA, et al. Lipid rafts and dopamine receptor signaling. Int J Mol Sci 2020;21(23):8909; doi: 10.3390/ijms21238909

McLaughlin M, Vandenbroeck K. The endoplasmic reticulum protein folding factory and its chaperones: New targets for drug discovery? Br J Pharmacol 2011;162(2):328–345; doi: 10.1111/j.1476-5381.2010.01064.x

Mittal M, Siddiqui MR, Tran K, et al. Reactive oxygen species in inflammation and tissue injury. Antioxid Redox Signal 2014;20(7):1126–1167; doi: 10.1089/ars.2012.5149

Oğuz N, Kırça M, Çetin A, et al. Effect of uric acid on inflammatory COX-2 and ROS pathways in vascular smooth muscle cells. J Recept Signal Transduct Res 2017;37(5):500–505; doi: 10.1080/10799893.2017.1360350

Qaddumi WN, Jose PA. The role of the renal dopaminergic system and oxidative stress in the pathogenesis of hypertension. Biomedicines 2021;9(2):139; doi: 10.3390/biomedicines9020139

Quiroz Y, Bravo J, Herrera-Acosta J, et al. Apoptosis and NFκB activation are simultaneously induced in renal tubulointerstitium in experimental hypertension. Kidney Int Suppl 2003; (86):S27–S32.; doi: 10.1046/j.1523-1755.64.s86.6.x

Ramming T, Okumura M, Kanemura S, et al. A PDI-catalyzed thiol-disulfide switch regulates the production of hydrogen peroxide by human Ero1. Free Radic Biol Med 2015;83:361–372; doi: 10.1016/j.freeradbiomed.2015.02.011

Rong G, Tang X, Guo T, et al. Advanced oxidation protein products induce apoptosis in podocytes through induction of endoplasmic reticulum stress. J Physiol Biochem 2015;71(3): 455–470; doi: 10.1007/s13105-015-0424-x

Sanada H, Jose PA, Hazen-Martin D, et al. Dopamine-1 receptor coupling defect in renal proximal tubule cells in hypertension. Hypertension 1999;33(4):1036–1042; doi: 10.1161/01.hyp.33.4.1036

Sauvageau E, Rochdi MD, Oueslati M, et al. CNIH4 interacts with newly synthesized GPCR and controls their export from the endoplasmic reticulum. Traffic 2014;15(4):383–400; doi: 10.1111/tra.12148

Schrag JD, Bergeron JJ, Li Y, et al. The structure of calnexin, an ER chaperone involved in quality control of protein folding. Mol Cell 2001;8(3):633–644; doi: 10.1016/s1097-2765(01)00318-5

Shi Y, Tian C, Yu X, et al. Protective effects of *Smilax glabra Roxb*. against lead-induced renal oxidative stress, inflammation and apoptosis in weaning rats and HEK-293 cells. Front Pharmacol 2020;11:556248; doi: 10.3389/fphar.2020.556248

Singh A, Kukreti R, Saso L, et al. Oxidative stress: A key modulator in neurodegenerative diseases. Molecules 2019a; 24(8):1583; doi: 10.3390/molecules24081583

Singh R, Letai A, Sarosiek K. Regulation of apoptosis in health and disease: The balancing act of BCL-2 family proteins. Nat Rev Mol Cell Biol 2019b;20(3):175–193; doi: 10.1038/s41580-018-0089-8

Stoelting M, Geyer M, Reuter S, et al. Alpha/beta hydrolase 1 is upregulated in D5 dopamine receptor knockout mice and reduces O2- production of NADPH oxidase. Biochem Biophys Res Commun 2009;379(1):81–85; doi: 10.1016/j.bbrc.2008.12.008

Sun Y, Rombola C, Jyothikumar V, et al. Förster resonance energy transfer microscopy and spectroscopy for localizing protein-protein interactions in living cells. Cytometry A 2013; 83(9):780–793. doi: 10.1002/cyto.a.22321

Sun Y, Rawish E, Nording HM, et al. Inflammation in metabolic and cardiovascular disorders-role of oxidative stress. Life 2021;11(7):672; doi: 10.3390/life11070672

Tayebati SK, Lokhandwala MF, Amenta F. Dopamine and vascular dynamics control: Present status and future perspectives. Curr Neurovasc Res 2011;8(3):246–257; doi: 10.2174/156720211796558032

Tice MA, Hashemi T, Taylor LA, et al. Characterization of the binding of SCH 39166 to the five cloned dopamine receptor subtypes. Pharmacol Biochem Behav 1994;49(3):567–571; doi: 10.1016/0091-3057(94)90070-1

Undieh AS. Pharmacology of signaling induced by dopamine D1-like receptor activation. Pharmacol Ther 2010;128(1):37–60; doi: 10.1016/j.pharmthera.2010.05.003

Valero Y, Martínez-Morcillo FJ, Esteban MÁ, et al. Fish peroxiredoxins and their role in immunity. Biology 2015;4(4): 860–880; doi: 10.3390/biology4040860

Wang X, Luo Y, Escano CS, et al. Upregulation of renal sodium transporters in D5 dopamine receptor-deficient mice. Hypertension 2010;55(6):1431–1437; doi: 10.1161/HYPERTENSIONAHA.109.148643

Wang S, Tan X, Chen P, et al. Role of thioredoxin 1 in impaired renal sodium excretion of hD_5R F173L transgenic mice. J Am Heart Assoc 2019;8(8):e012192; doi: 10.1161/JAHA.119.012192

Wang HY, Bharti D, Levental I. Membrane heterogeneity beyond the plasma membrane. Front Cell Dev Biol 2020;8: 580814; doi: 10.3389/fcell.2020.580814

Wilcox CS. Effects of tempol and redox-cycling nitroxides in models of oxidative stress. Pharmacol Ther 2010;126(2):119–145; doi: 10.1016/j.pharmthera.2010.01.003

Xiao J, Zhang XL, Fu C, et al. Soluble uric acid increases NALP3 inflammasome and interleukin-1β expression in human primary renal proximal tubule epithelial cells through the Toll-like receptor 4-mediated pathway. Int J Mol Med 2015;35(5):1347–1354; doi: 10.3892/ijmm.2015.2148

Xiao L, Harrison DG. Inflammation in hypertension. Can J Cardiol 2020;36(5):635–647; doi: 10.1016/j.cjca.2020.01.013

Xiong W, Meng XF, Zhang C. NLRP3 Inflammasome in metabolic-associated kidney diseases: An update. Front Immunol 2021;12:714340; doi: 10.3389/fimmu.2021.714340

Yamada S, Guo X. Peroxiredoxin 4 (PRDX4): Its critical in vivo roles in animal models of metabolic syndrome ranging from atherosclerosis to nonalcoholic fatty liver disease. Pathol Int 2018;68(2):91–101; doi: 10.1111/pin.12634

Yang Z, Asico LD, Yu P, et al. D5 dopamine receptor regulation of reactive oxygen species production, NADPH oxidase, and blood pressure. Am J Physiol Regul Integr Comp Physiol 2006;290(1):R96–R104; doi: 10.1152/ajpregu.00434.2005

Yang S, Yang Y, Yu P, et al. Dopamine D1 and D5 receptors differentially regulate oxidative stress through paraoxonase 2 in kidney cells. Free Radic Res 2015;49(4):397–410; doi: 10.3109/10715762.2015.1006215

Yu P, Sun M, Villar VA, et al. Differential dopamine receptor subtype regulation of adenylyl cyclases in lipid rafts in human embryonic kidney and renal proximal tubule cells. Cell Signal 2014;26(11):2521–2529; doi: 10.1016/j.cellsig.2014.07.003

Zeng C, Villar VA, Yu P, et al. Reactive oxygen species and dopamine receptor function in essential hypertension. Clin Exp Hypertens 2009;31(2):156–178; doi: 10.1080/10641960802621283

Zhang MZ, Harris RC. Antihypertensive mechanisms of intrarenal dopamine. Curr Opin Nephrol Hypertens 2015;24(2): 117–122; doi: 10.1097/MNH.0000000000000104

Address correspondence to:
Dr. Hewang Lee
Department of Medicine
The George Washington University
School of Medicine & Health Sciences
2300 Eye Street, NW
Washington, DC 20052
USA

E-mail: lih@gwu.edu

Date of first submission to ARS Central, March 15, 2022; date of final revised submission, November 5, 2022; date of acceptance, November 5, 2022.

Abbreviations Used

AMPA = α-amino-3-hydroxy-5-methyl-4-isoxazolepropionic acid
ANOVA = analysis of variance
cAMP = 3',5'-cyclic adenosine monophosphate
Cas9 = CRISPR-associated protein 9
CHOP = CCAAT/enhancer-binding protein-homologous protein
CNIH4 = cornichon family AMPA receptor auxiliary protein 4
CRISPR = clustered regularly interspaced short palindromic repeats
D_1R = dopamine D1 receptor
D_5R = dopamine D5 receptor
Drd5 = D_5R gene
ELISA = enzyme-linked immunosorbent assay
ER = endoplasmic reticulum
FBS = fetal bovine serum
FEN = fenoldopam
FLIM = fluorescence lifetime imaging microscopy
FRET = fluorescence (Förster) resonance energy transfer
GAPDH = glyceraldehyde 3-phosphate dehydrogenase
GPCR = G protein-coupled receptor
HEK293 = human embryonic kidney 293
hRPTC = human renal proximal tubule cell
IL = interleukin
IRE1α = inositol-requiring transmembrane kinase/endoribonuclease 1α
JNK = c-Jun N-terminal kinases
LR = lipid raft
LSM = laser scanning microscope
M-β-CD = methyl-β-cyclodextrin
NADPH = nicotinamide adenine dinucleotide phosphate
NF-κB = nuclear factor kappa-light-chain-enhancer of activated B cells
NHE3 = sodium-hydrogen exchanger 3 or solute carrier family 9 member A3
NLRP3 = nucleotide-binding oligomerization domain, leucine-rich repeat and pyrin domain-containing-3
non-LR = non-lipid raft
PBS = phosphate-buffered saline
PERK = protein kinase RNA-like endoplasmic reticulum kinase
PKA = protein kinase A
PRDX = peroxiredoxin
ROI = regions of interest
ROS = reactive oxygen species
SCH = SCH 39166
SDS-PAGE = sodium dodecyl sulfate-polyacrylamide gel electrophoresis
TNF = tumor necrosis factor
VEH = vehicle